

# Fractional Programming for Kullback-Leibler Divergence in Hypothesis Testing

Jeongwoo Park, Seongkyu Jung, Kaiming Shen, and Jeonghun Park

**Abstract**—Maximizing the Kullback-Leibler divergence (KLD) is a fundamental problem in waveform design for active sensing and hypothesis testing, as it directly relates to the error exponent of detection probability. However, the associated optimization problem is highly nonconvex due to the intricate coupling of log-determinant and matrix trace terms. Existing solutions often suffer from high computational complexity, typically requiring matrix inversion at every iteration. In this paper, we propose a computationally efficient optimization framework based on fractional programming (FP). Our key idea is to reformulate the KLD maximization problem into a sequence of tractable quadratic subproblems using matrix FP. To further reduce complexity, we introduce a nonhomogeneous relaxation technique that replaces the costly linear system solver with a simple closed-form update, thereby reducing the per-iteration complexity to quadratic order. To compensate for the convergence speed trade-off caused by relaxation, we employ an acceleration method called STEM by interpreting the iterative scheme as a fixed-point mapping. The resulting algorithm achieves significantly faster convergence rates with low per-iteration cost. Numerical results demonstrate that our approach reduces the total runtime by orders of magnitude compared to a state-of-the-art benchmark. Finally, we apply the proposed framework to a multiple random access scenario and a joint integrated sensing and communication scenario, validating the efficacy of our framework in such applications.

## I. INTRODUCTION

Kullback–Leibler divergence (KLD), also known as relative entropy, quantifies the amount of dissimilarity between two probability distributions [1]. As a measure of how one distribution diverges from another in expectation, KLD plays a pivotal role in various formulations of information theory. For example, in mismatched source coding, KLD-related quantity, i.e., the cross-entropy, naturally characterizes the rate penalty incurred when encoding is performed under an incorrect source model [2]. In universal compression, KLD determines the redundancy rate when the encoder must operate without precise knowledge of the source distribution. In particular, considering hypothesis testing, which is the main focus of this paper, maximizing the KLD between the hypotheses directly enhances their statistical separability. According to the Chernoff–Stein lemma [3], the KLD dictates the error exponent

This work was supported in part by Institute of Information & Communications Technology Planning & Evaluation (IITP) grant funded by the Korea government (MSIT) (No. RS-2024-00397216, Development of the Upper-mid Band Extreme massive MIMO (E-MIMO), No. 2025-RS-2024-00428780, 6G Cloud Research and Education Open Hub and No. RS-2024-00434743, YKCS Open RAN Global Collaboration Center). J. Park, S. Jung and J. Park are with School of Electrical and Electronic Engineering, Yonsei University, Seoul, South Korea (e-mail: {samyffff, wjdtjd963, jhpark}@yonsei.ac.kr). K. Shen is with School of Science and Engineering, The Chinese University of Hong Kong, Shenzhen, China (e-mail: shenkaiming@cuhk.edu.cn).

of the miss-detection probability under a fixed false-alarm constraint; hence, a larger KLD implies a faster exponential decay of detection errors. From this perspective, maximizing the KLD leads to sensing waveforms that maximize detection probability under given long-term statistics. Such designs directly determine the sensing system’s ability to reliably detect targets under practical resource constraints, e.g., sensing time, bandwidth, or power. Accordingly, the development of efficient KLD optimization techniques is of central importance in sensing systems.

The recent rise of integrated sensing and communication (ISAC) systems further intensifies the need for such efficient KLD design methods. Given that sensing and communication share spectrum, power, and also front-end hardware in ISAC, the transmit waveforms must be jointly designed to simultaneously optimize communication and sensing performance metrics. In this context, KLD is often employed as a sensing performance metric, while mutual information (MI) is typically used to characterize the achievable rates [4]–[6]. Such a joint design objective demands tractable and scalable optimization algorithms.

Unfortunately, however, the analytical form of the KLD is often very complicated, making direct optimization intractable. Even under the Gaussian assumption, which yields an explicit closed-form expression, the resulting optimization problem typically remains nonconvex due to the intricate coupling between the waveform parameters and the statistical structure of the received signal. This nonconvexity limits the applicability of conventional convex optimization techniques since neither global optimality nor reliable convergence properties can be guaranteed. In this paper, we propose a new optimization method for maximizing the KLD in hypothesis testing. Our key idea is to apply fractional programming (FP) [7], [8] to reformulate the problem into a sequence of concave subproblems, whereby each subproblem can be solved efficiently. We demonstrate that our method achieves superior performance compared to existing state-of-the-art methods, while significantly reducing computational complexity.

## A. Related Works

Prior works addressed the sensing waveform design problem primarily in the context of multi-input multi-output (MIMO) radar systems. Under this setup, existing studies predominantly focused on optimizing estimation-theoretic criteria or signal-to-interference-plus-noise ratio (SINR). For instance, [9] suggested shaping the probing signal covariance matrix to approximate a desired beampattern or to maximize the spatial

power at target locations, thereby enhancing the SINR. In [10], it was demonstrated that spatially orthogonal signal transmission minimizes the Cramér-Rao bound (CRB) for direction-of-arrival (DOA) estimation. These works primarily aim at sensing tasks formulated as parameter estimation problems. In [11], it was shown that maximizing the MI between the random target response and the received signal is equivalent to minimizing the mean-squared error (MSE) of the target response estimation.

However, distinguishing between hypotheses (i.e., detection) is fundamentally different from parameter estimation. For this reason, when the primary objective is detection, the adoption of KLD as a performance metric is rigorously motivated. The use of KLD for detection-centric waveform design originates from [12]. Therein, the locally most powerful (LMP) detector was derived under low SNR conditions, where the LMP detector is known to be optimal. It was shown that the detection performance of the LMP detector is strictly monotonic in the KLD, thereby establishing the KLD as a rigorous optimality criterion for target detection.

Nonetheless, practical optimization algorithms for KLD are much less sophisticated compared to those for other information-theoretic metrics, such as MI [7], [13]–[16]. While MI maximization has been extensively studied and often admits elegant closed-form solutions via water-filling algorithms [17], the analytical form of KLD for detection involves intricate log-determinant (log-det) and trace terms coupled with the waveform covariance, rendering KLD maximization highly nonconvex and intractable. To circumvent this intractability, earlier approaches relied on restrictive assumptions or heuristic designs. For instance, in [18], the authors considered optimizing parameters for the fixed waveform structure (e.g., chirp rate or pulse width) to improve resolvability, rather than optimizing the waveform structure itself. Similarly, [19] derived analytical solutions for space-time codes, but their validity was limited to specific spectral conditions or global energy constraints.

Efforts to address general nonconvex KLD problems without such restrictions have focused on numerical optimization techniques. [20] modeled the problem as sequential multi-hypothesis testing and employed semi-definite relaxation (SDR) to handle the nonconvex constraints. While effective, SDR-based methods suffer from high computational complexity and require randomization steps to recover rank-1 solutions. The current state of the art is represented by [21], which applied the minorization-maximization (MM) framework. Although its quadratic minorizer reduces the per-iteration complexity compared to previous approaches [22] proposed by the same authors, it still necessitates solving a large-scale linear system at each iteration, which imposes a cubic computational burden that restricts scalability for large antenna arrays.

The absence of a computationally efficient solver has limited the application of KLD in the emerging field of ISAC. In ISAC systems, the transmit waveform is designed to jointly maximize a communication metric—typically MI—alongside a sensing metric. For sensing metrics such as CRB or beam-pattern MSE, numerous ISAC waveform design approaches have been developed. For instance, [23] considered minimizing the CRB for target estimation under SINR constraints, while

[24], [25] investigated joint waveform designs that maximize the sum communication MI while minimizing the beampattern MSE to form suitable sensing beams. However, efficient ISAC waveform design with KLD as the sensing metric remains challenging due to the lack of a tractable optimization framework for KLD maximization.

### B. Contributions

We propose a novel optimization framework to address KLD maximization. Our key idea is to reformulate the intricate Gaussian KLD objective using FP [13], thereby enabling the development of an algorithm that guarantees monotonic convergence with significantly reduced computational complexity. The main contributions are summarized as follows:

- We reformulate the nonconvex Gaussian KLD objective by applying matrix FP techniques to the log-det term and the trace term. This approach decouples the matrix inverse from the design variables, transforming the original problem into a sequence of concave quadratic subproblems. This reformulation exploits the structure of KLD to provide a tight surrogate function that guarantees monotonic convergence.
- To overcome the cubic complexity of solving linear systems in the FP approach, we introduce a nonhomogeneous relaxation technique. By replacing the anisotropic curvature of the surrogate with a conservative isotropic bound, we derive a closed-form waveform update with quadratic complexity. This significantly enhances scalability while strictly preserving the monotonic ascent property.
- We develop an accelerated optimization framework, termed A-MM-KLD, by interpreting the iterative algorithm as a fixed-point mapping and incorporating a Steffensen-type acceleration. In this scheme, the accelerator approximates the Jacobian to achieve a quadratic convergence rate. This synergy effectively compensates for the increased iteration count caused by the relaxed surrogate, resulting in a substantial reduction in total runtime compared to a state-of-the-art baseline.
- We demonstrate that our framework is applicable to several practical scenarios, including ISAC and multiple random access scenarios. In the ISAC case, leveraging the fact that MI maximization via FP is well established [7], [26], we show that our proposed framework can be seamlessly integrated to jointly maximize the composite objective of MI and KLD. In the multiple random access scenario, formulated as maximizing a weighted sum of Gaussian KLDs, each term in the objective preserves the single-Gaussian algebraic form, ensuring that our method can be suitably applied.

### C. Notations

Boldface lower-case and upper-case letters denote column vectors and matrices, respectively. The set of  $m$ -dimensional complex vectors and  $m \times n$  complex matrices are denoted by  $\mathbb{C}^m$  and  $\mathbb{C}^{m \times n}$ , while  $\mathbb{H}_+$  and  $\mathbb{H}_{++}$  represent the sets of Hermitian positive semi-definite (PSD) and positive definite

(PD) matrices, respectively, where the superscript  $n$ , if specified, denotes the matrix dimension  $n \times n$ . For a matrix  $\mathbf{A}$ ,  $\mathbf{A}^T$ ,  $\mathbf{A}^H$ , and  $|\mathbf{A}|$  denote its transpose, Hermitian transpose and determinant, whereas  $\|\mathbf{a}\|$  denotes the Euclidean norm of a vector  $\mathbf{a}$ . The notation  $\mathbf{I}_n$  refers to the  $n \times n$  identity matrix, and  $\mathbf{0}$  denotes the all-zero vector or matrix, where the subscript is omitted when the dimension is evident from the context. The operators  $\text{vec}(\cdot)$ ,  $\otimes$ ,  $\langle \cdot, \cdot \rangle$ , and  $\Re\{\cdot\}$  correspond to the vectorization, Kronecker product, inner product, and the real part of a complex argument, respectively. In terms of matrix inequalities,  $\mathbf{A} \succeq \mathbf{B}$  (or  $\mathbf{A} \succ \mathbf{B}$ ) implies that  $\mathbf{A} - \mathbf{B}$  is PSD (or PD). Finally,  $\mathbb{E}_{\mathbf{X}}[\cdot]$  denotes the expectation with respect to the random variables  $\mathbf{X}$ , and  $\mathcal{CN}(\mathbf{0}, \mathbf{R})$  denotes the zero-mean circularly symmetric complex Gaussian distribution with covariance matrix  $\mathbf{R}$ , whose probability density function (PDF) is denoted by  $p_{\mathcal{CN}}(\mathbf{x}; \mathbf{R})$ .

## II. SYSTEM MODEL AND PROBLEM FORMULATION

We consider a MIMO system in which sensing signals are transmitted from  $N_t$  transmit antennas and the echo signals are received by  $N_r$  receive antennas. We use  $T$  snapshots for sensing, each representing an independent observation. The target response matrix is denoted by  $\mathbf{H} \in \mathbb{C}^{N_t \times N_r}$ .

To detect the presence or absence of a target, we formulate a binary hypothesis testing problem based on the observed sensing signal returns. The hypotheses are given by:

$$\mathcal{H}_0 : \mathbf{Y} = \mathbf{X}\mathbf{C}_0 + \mathbf{N}, \quad (1)$$

$$\mathcal{H}_1 : \mathbf{Y} = \mathbf{X}\mathbf{H} + \mathbf{X}\mathbf{C}_1 + \mathbf{N}, \quad (2)$$

where  $\mathbf{Y} \in \mathbb{C}^{T \times N_r}$  is the observation matrix collected over  $T$  snapshots across  $N_r$  receive antennas,  $\mathbf{X} \in \mathbb{C}^{T \times N_t}$  represents the transmitted signal matrix and  $\mathbf{N} \in \mathbb{C}^{T \times N_r}$  is the additive noise matrix. The matrices  $\mathbf{C}_0$  and  $\mathbf{C}_1$  denote the clutter responses under  $\mathcal{H}_0$  and  $\mathcal{H}_1$ , respectively. This formulation accommodates general scenarios by allowing for distinct clutter responses ( $\mathbf{C}_0 \neq \mathbf{C}_1$ ). Nevertheless, the proposed method remains applicable without modification for the special case of identical clutter responses, where  $\mathbf{C}_0 = \mathbf{C}_1$ .

Assuming that the receive antennas are sufficiently separated, the columns of the random matrices  $\mathbf{H}$ ,  $\mathbf{C}_0$ ,  $\mathbf{C}_1$ , and  $\mathbf{N}$  are modeled as mutually independent and identically distributed (i.i.d.) zero-mean complex Gaussian vectors. The covariance matrices  $\mathbf{R}_H$ ,  $\mathbf{R}_0$ ,  $\mathbf{R}_1$ , and  $\mathbf{R}_N$  represent the spatial statistics of the target response, clutter under  $\mathcal{H}_0$ , clutter under  $\mathcal{H}_1$ , and noise, respectively. We note that this assumption follows the standard modeling practice in MIMO radar literature [27], [28].

The primary objective in the hypothesis testing (1), (2) is to reliably distinguish between the absence ( $\mathcal{H}_0$ ) and presence ( $\mathcal{H}_1$ ) of the target. According to the Neyman–Pearson criterion [29], the optimal detector is the likelihood-ratio test (LRT), given by:

$$\Lambda(\mathbf{Y}) = \frac{p(\mathbf{Y}|\mathcal{H}_1)}{p(\mathbf{Y}|\mathcal{H}_0)} \stackrel{\mathcal{H}_1}{\gtrless} \eta, \quad (3)$$

where  $\eta$  is a threshold chosen based on the desired probability of false alarm or detection, and  $p(\mathbf{Y}|\mathcal{H}_1)$  and  $p(\mathbf{Y}|\mathcal{H}_0)$  denote

the likelihood functions under the respective hypotheses. These likelihood functions are given by:

$$p(\mathbf{Y}|\mathcal{H}_i) = \frac{1}{(\pi^T |\mathbf{K}_i|)^{N_r}} \exp\left(-\bar{\mathbf{y}}^H (\mathbf{I}_{N_r} \otimes \mathbf{K}_i)^{-1} \bar{\mathbf{y}}\right), \quad i = 0, 1, \quad (4)$$

where

$$\bar{\mathbf{y}} = \text{vec}(\mathbf{Y}) \in \mathbb{C}^{N_r T}, \quad (5)$$

$$\mathbf{K}_0 = \mathbf{X}\mathbf{R}_0\mathbf{X}^H + \mathbf{R}_N, \quad (6)$$

$$\mathbf{K}_1 = \mathbf{X}\mathbf{R}_H\mathbf{X}^H + \mathbf{R}_N, \quad (7)$$

$$\mathbf{R}_H = \mathbf{R}_H + \mathbf{R}_1. \quad (8)$$

The asymptotic performance of the LRT is characterized by the Chernoff–Stein lemma, which relates the exponential decay rate of the type-II error (miss-detection) probability to the KLD divergence [30]. Specifically, letting  $\alpha$  denote the fixed type-I error (false-alarm) probability, the minimum achievable type-II error probability, denoted by  $\beta_T(\alpha)$ , decays as characterized by

$$\lim_{T \rightarrow \infty} \frac{1}{T} \log \beta_T(\alpha) = -D_{\text{KL}}(\mathbf{Y}_0 \parallel \mathbf{Y}_1), \quad (9)$$

where  $D_{\text{KL}}(\cdot \parallel \cdot)$  denotes the KLD. To be specific, the KLD  $D_{\text{KL}}(\mathbf{Y}_0 \parallel \mathbf{Y}_1)$  is defined as

$$\begin{aligned} D_{\text{KL}}(\mathbf{Y}_0 \parallel \mathbf{Y}_1) &= -\mathbb{E}_{\mathbf{Y} \mid \mathcal{H}_0} \left[ \log \frac{p(\mathbf{Y}|\mathcal{H}_1)}{p(\mathbf{Y}|\mathcal{H}_0)} \right] \\ &= N_r \left( \log |\mathbf{K}_0^{-1} \mathbf{K}_1| + \text{Tr}(\mathbf{K}_1^{-1} \mathbf{K}_0) \right) - N_r T, \end{aligned} \quad (10)$$

where  $\mathbf{Y}_0$  and  $\mathbf{Y}_1$  denote the signals received under  $\mathcal{H}_0$  and  $\mathcal{H}_1$ , respectively. As such, when the number of snapshots is sufficiently large (i.e.,  $T > \max\{N_r, N_t\}$ ), in order to reduce the type-II error, it is desirable to design the transmit waveform  $\mathbf{X}$  such that

$$\begin{aligned} &\underset{\mathbf{X}}{\text{maximize}} \quad D_{\text{KL}}(\mathbf{Y}_0 \parallel \mathbf{Y}_1), \\ &\text{subject to} \quad \text{Tr}(\mathbf{X}\mathbf{X}^H) \leq P_t. \end{aligned} \quad (11)$$

Here,  $P_t$  is the transmit power constraint. This paper primarily focuses on addressing (11).

Ignoring a constant term, the objective of the considered problem (11) can be specified

$$f(\mathbf{X}) = \log |\mathbf{K}_0^{-1} \mathbf{K}_1| + \text{Tr}(\mathbf{K}_1^{-1} \mathbf{K}_0). \quad (12)$$

This depends on the design variable  $\mathbf{X}$  through  $\mathbf{K}_0 = \mathbf{X}\mathbf{R}_0\mathbf{X}^H + \mathbf{R}_N$  and  $\mathbf{K}_1 = \mathbf{X}\mathbf{R}_H\mathbf{X}^H + \mathbf{R}_N$ , which are quadratic in  $\mathbf{X}$ . Thus, concavity/convexity of the log-det and trace functions is lost when they are composed with  $\mathbf{X}$ . In particular, the coupling term  $\text{Tr}(\mathbf{K}_1^{-1} \mathbf{K}_0)$  introduces a quadratic dependence on  $\mathbf{X}$ , making the Hessian indefinite. For instance, even considering the scalar case, the objective function has the form of

$$f(x) = \log \frac{bx^2 + \sigma^2}{ax^2 + \sigma^2} + \frac{ax^2 + \sigma^2}{bx^2 + \sigma^2}, \quad (13)$$

which is neither convex nor concave in  $x$ . Together with practical power or structure constraints, the problem becomes a highly nonconvex program, where typical optimization methods are not applicable. In the next section, we address this by proposing a FP-based optimization technique.

### III. PROPOSED FP-BASED KLD OPTIMIZATION

In this section, we present our main method to solve (11). We begin by rewriting the objective function (12) as

$$\begin{aligned} f(\mathbf{X}) &= \log|\mathbf{K}_0^{-1}\mathbf{K}_1| + \text{Tr}(\mathbf{K}_1^{-1}\mathbf{K}_0) \\ &= \log|\mathbf{I}_T + \mathbf{K}_0^{-1}\mathbf{X}(\mathbf{R}_{H1} - \mathbf{R}_0)\mathbf{X}^H| \\ &\quad - \text{Tr}(\mathbf{K}_1^{-1}\mathbf{X}(\mathbf{R}_{H1} - \mathbf{R}_0)\mathbf{X}^H). \end{aligned} \quad (14)$$

Without loss of generality, we assume  $\mathbf{R}_{H1} - \mathbf{R}_0 \succ 0$  [31]. This is a natural condition in binary detection problems: under  $\mathcal{H}_1$ , an additional signal component is present compared to  $\mathcal{H}_0$ , which necessarily enlarges the covariance matrix. If this condition did not hold, the two hypotheses would not be distinguishable, and the detection problem would be ill-posed. In particular, if the clutter response is identical under both hypotheses ( $\mathbf{C}_0 = \mathbf{C}_1$ ), we have

$$\mathbf{R}_{H1} - \mathbf{R}_0 = \mathbf{R}_H \succ 0, \quad (15)$$

thereby the condition holds naturally.

With the above assumption, it admits a Cholesky factorization,  $\mathbf{R}_{H1} - \mathbf{R}_0 = \mathbf{L}\mathbf{L}^H$ . Using this, the objective becomes

$$f(\mathbf{X}) = \log|\mathbf{I}_{N_t} + (\mathbf{X}\mathbf{L})^H\mathbf{K}_0^{-1}(\mathbf{X}\mathbf{L})| - \text{Tr}((\mathbf{X}\mathbf{L})^H\mathbf{K}_1^{-1}(\mathbf{X}\mathbf{L})). \quad (16)$$

Still, however, (16) contains matrix-ratio terms inside both the log-det and the trace. To address this challenge, we introduce auxiliary variables and apply a sequence of matrix transformations, each leading to a tractable surrogate. We note that our approach is rooted in the principles of matrix FP [13], [26], [32]. We provide further clarification regarding the connection between the applied FP and the MM framework in Remark 1.

At first, to handle the challenging log-det term in (16), we apply the matrix Lagrangian dual transform [13]. This transform provides a tight and global lower bound on the log-det function.

**Lemma 1** (Matrix Lagrangian dual transform [13]). *Let  $\mathbf{Q}, \mathbf{\Gamma} \succeq \mathbf{0}$  and define  $\mathbf{Z} = \mathbf{I} + \mathbf{Q} \succ \mathbf{0}$ ,  $\mathbf{U} = \mathbf{I} + \mathbf{\Gamma} \succ \mathbf{0}$ . Then*

$$\log|\mathbf{I} + \mathbf{Q}| \geq \log|\mathbf{I} + \mathbf{\Gamma}| + \text{Tr}(\mathbf{I}) - \text{Tr}((\mathbf{I} + \mathbf{\Gamma})(\mathbf{I} + \mathbf{Q})^{-1}), \quad (17)$$

with equality if and only if  $\mathbf{Q} = \mathbf{\Gamma}$ .

*Proof sketch.* The inequality follows from the basic bound

$$\log|\mathbf{M}| \leq \text{Tr}(\mathbf{M}) - \text{Tr}(\mathbf{I}) \quad (\mathbf{M} \succ \mathbf{0}), \quad (18)$$

with equality if and only if  $\mathbf{M} = \mathbf{I}$ . When  $\mathbf{M} = \mathbf{U}\mathbf{Z}^{-1}$ , we have

$$\log|\mathbf{U}\mathbf{Z}^{-1}| \leq \text{Tr}(\mathbf{U}\mathbf{Z}^{-1}) - \text{Tr}(\mathbf{I}). \quad (19)$$

Rearranging gives

$$\log|\mathbf{Z}| \geq \log|\mathbf{U}| + \text{Tr}(\mathbf{I}) - \text{Tr}(\mathbf{U}\mathbf{Z}^{-1}). \quad (20)$$

Substituting  $\mathbf{Z} = \mathbf{I} + \mathbf{Q}$ ,  $\mathbf{U} = \mathbf{I} + \mathbf{\Gamma}$  completes the proof. ■

Applying Lemma 1 to the first term in (16), we get

$$\begin{aligned} \log|\mathbf{I}_{N_t} + (\mathbf{X}\mathbf{L})^H\mathbf{K}_0^{-1}(\mathbf{X}\mathbf{L})| \\ \geq \log|\mathbf{I}_{N_t} + \mathbf{\Gamma}| + \text{Tr}(\mathbf{I}_{N_t}) \\ - \text{Tr}((\mathbf{I}_{N_t} + \mathbf{\Gamma})(\mathbf{I}_{N_t} + (\mathbf{X}\mathbf{L})^H\mathbf{K}_0^{-1}(\mathbf{X}\mathbf{L}))^{-1}). \end{aligned} \quad (21)$$

By modifying the final trace term of inequality (21) using the Woodbury matrix identity [33] and combining the second term from (16), we obtain an equivalent reformulation of the problem. This introduces an auxiliary variable  $\mathbf{\Gamma} \in \mathbb{H}_+^{N_t}$  and yields a new surrogate for the original objective function, resulting in the formulation in (22).

$$\begin{aligned} &\underset{\mathbf{X}, \mathbf{\Gamma}}{\text{maximize}} \quad f_\ell(\mathbf{X}, \mathbf{\Gamma}) \\ &\text{subject to} \quad \text{Tr}(\mathbf{X}\mathbf{X}^H) \leq P_t, \end{aligned} \quad (22)$$

where

$$f_\ell(\mathbf{X}, \mathbf{\Gamma}) = \log|\mathbf{I}_{N_t} + \mathbf{\Gamma}| - \text{Tr}(\mathbf{\Gamma}) + \text{Tr}(\mathbf{\Gamma}(\mathbf{X}\mathbf{L})^H\mathbf{K}_1^{-1}(\mathbf{X}\mathbf{L})). \quad (23)$$

This transformation effectively decouples the matrix inverse from the log-det operator, resulting in a more tractable structure. In particular, by selecting an appropriate auxiliary variable  $\mathbf{\Gamma}$  at each iteration, we obtain a suitable surrogate function  $f_\ell$ , which achieves a tight lower bound of the original objective at the current point as stated in Lemma 1. Specifically, by its equality condition, this tight bound is achieved when:

$$\mathbf{\Gamma}^* = (\mathbf{X}\mathbf{L})^H\mathbf{K}_0^{-1}(\mathbf{X}\mathbf{L}). \quad (24)$$

However,  $f_\ell$  in (23) remains intractable due to the matrix inverse in the trace term. To deal with this, we further apply the following lemma.

**Lemma 2** (Matrix quadratic transform [13]). *Let  $\mathbf{A} \in \mathbb{H}_+$  and  $\mathbf{B} \in \mathbb{H}_{++}$ . Then for any  $\mathbf{\Psi}$ ,*

$$\text{Tr}(\sqrt{\mathbf{A}}^H\mathbf{B}^{-1}\sqrt{\mathbf{A}}) \geq 2\Re\{\text{Tr}(\mathbf{\Psi}^H\sqrt{\mathbf{A}})\} - \text{Tr}(\mathbf{\Psi}^H\mathbf{B}\mathbf{\Psi}), \quad (25)$$

where  $\mathbf{A} = \sqrt{\mathbf{A}}\sqrt{\mathbf{A}}^H$ , with equality if and only if  $\mathbf{\Psi} = \mathbf{B}^{-1}\sqrt{\mathbf{A}}$ .

*Proof sketch.* Consider the matrix  $\mathbf{Z}$  defined as

$$\mathbf{Z} = (\mathbf{\Psi} - \mathbf{B}^{-1}\sqrt{\mathbf{A}})^H\mathbf{B}(\mathbf{\Psi} - \mathbf{B}^{-1}\sqrt{\mathbf{A}}) \quad (26)$$

Since  $\mathbf{B}$  is PD,  $\mathbf{Z}$  is a PSD matrix.

$$\begin{aligned} \mathbf{Z} &= (\mathbf{\Psi} - \mathbf{B}^{-1}\sqrt{\mathbf{A}})^H\mathbf{B}(\mathbf{\Psi} - \mathbf{B}^{-1}\sqrt{\mathbf{A}}) \\ &= \mathbf{\Psi}^H\mathbf{B}\mathbf{\Psi} - 2\Re\{\mathbf{\Psi}^H\sqrt{\mathbf{A}}\} + \sqrt{\mathbf{A}}^H\mathbf{B}^{-1}\sqrt{\mathbf{A}} \succeq \mathbf{0} \end{aligned} \quad (27)$$

with equality if and only if  $\mathbf{\Psi} - \mathbf{B}^{-1}\sqrt{\mathbf{A}} = \mathbf{0}$ . ■

Lemma 2 enables us to reformulate the matrix inverse term as an equivalent quadratic optimization with a new auxiliary variable  $\mathbf{\Psi} \in \mathbb{C}^{T \times N_t}$ . By applying this transformation, we arrive at the final surrogate objective:

$$\begin{aligned} &\underset{\mathbf{X}, \mathbf{\Gamma}, \mathbf{\Psi}}{\text{maximize}} \quad f_q(\mathbf{X}, \mathbf{\Gamma}, \mathbf{\Psi}) \\ &\text{subject to} \quad \text{Tr}(\mathbf{X}\mathbf{X}^H) \leq P_t, \end{aligned} \quad (28)$$

where

$$\begin{aligned} f_q(\mathbf{X}, \mathbf{\Gamma}, \mathbf{\Psi}) &= \log|\mathbf{I}_{N_t} + \mathbf{\Gamma}| - \text{Tr}(\mathbf{\Gamma}) \\ &\quad + \text{Tr}(2\Re\{(\mathbf{X}\mathbf{L})^H\mathbf{\Psi}\mathbf{\Gamma}\}) - \mathbf{\Psi}^H\mathbf{K}_1\mathbf{\Psi}\mathbf{\Gamma} \\ &= \underbrace{\log|\mathbf{I}_{N_t} + \mathbf{\Gamma}| - \text{Tr}(\mathbf{\Gamma}) - \text{Tr}(\mathbf{\Psi}^H\mathbf{R}_N\mathbf{\Psi}\mathbf{\Gamma})}_{\text{constant in } \mathbf{X}} \\ &\quad + 2\Re\{\text{Tr}(\mathbf{\Gamma}\mathbf{\Psi}^H\mathbf{X}\mathbf{L})\} - \text{Tr}(\mathbf{X}\mathbf{R}_{H1}\mathbf{X}^H\mathbf{\Psi}\mathbf{\Gamma}\mathbf{\Psi}^H). \end{aligned} \quad (29)$$

**Algorithm 1:** FP-KLD (Matrix FP + Quadratic Transform)

---

```

1 Input:  $P_t, \epsilon > 0$ ,  $t_{\max}$ ,  $\mathbf{R}_{H1}, \mathbf{R}_0, \mathbf{R}_N$ , and  $\mathbf{X}_{\text{init}}$ 
2 Precompute:  $\mathbf{R}_{H1} - \mathbf{R}_0 = \mathbf{L}\mathbf{L}^H$ 
3 Initialize:  $\mathbf{X}^{(0)} \leftarrow \mathbf{X}_{\text{init}}$ ; set  $t \leftarrow 0$ 
4 while  $t < t_{\max}$  do
5   Compute  $\mathbf{K}_0$  by (6) and  $\mathbf{K}_1$  by (7).
6   Update  $\mathbf{\Gamma}^{(t+1)}$  by (24).
7   Update  $\mathbf{\Psi}^{(t+1)}$  by (30).
8   Update  $\mathbf{X}^{(t+1)}$  by solving (32)
9   if  $\frac{f(\mathbf{X}^{(t+1)}) - f(\mathbf{X}^{(t)})}{f(\mathbf{X}^{(t)})} < \epsilon$  then
10    | break
11   end
12    $t \leftarrow t + 1$ 
13 end
14 Output:  $\mathbf{X}^* \leftarrow \mathbf{X}^{(t+1)}$ .

```

---

We note that the optimal choice for the auxiliary variable  $\mathbf{\Psi}$  that satisfies the equality in Lemma 2 is:

$$\mathbf{\Psi}^* = \mathbf{K}_1^{-1} \mathbf{X} \mathbf{L}. \quad (30)$$

With  $\mathbf{\Gamma}$  and  $\mathbf{\Psi}$  fixed at the corresponding iteration, the dependence on  $\mathbf{X}$  arises through the last two terms. Notably, since  $\mathbf{R}_{H1}$  and  $\mathbf{\Psi} \mathbf{\Gamma}^H$  are both PSD,  $f_q$  is a concave quadratic form with respect to  $\mathbf{X}$ ; thus the global optimal solution under the convex constraint can be obtained by solving the KKT conditions of the associated Lagrangian [34]. Specifically, we introduce a Lagrange multiplier  $\mu \geq 0$  for the power constraint and define the Lagrangian function as:

$$\mathcal{L}(\mathbf{X}, \mu) = f_q(\mathbf{X}, \mathbf{\Gamma}, \mathbf{\Psi}) - \mu(\text{Tr}(\mathbf{X}\mathbf{X}^H) - P_t). \quad (31)$$

By deriving the stationary condition, i.e., setting the gradient of  $\mathcal{L}$  to zero, we obtain a Sylvester-type equation [35], [36], given by:

$$\mathbf{A} \mathbf{X} \mathbf{R}_{H1} + \mu \mathbf{X} = \mathbf{B}, \quad (32)$$

where  $\mathbf{A} = \mathbf{\Psi} \mathbf{\Gamma} \mathbf{\Psi}^H$ ,  $\mathbf{B} = \mathbf{\Psi} \mathbf{\Gamma} \mathbf{L}^H$ . (32) can be solved by vectorizing it into a standard linear system:  $(\bar{\mathbf{A}} + \mu \mathbf{I}_{N_t T}) \bar{\mathbf{x}} = \bar{\mathbf{b}}$ , with  $\bar{\mathbf{x}} = \text{vec}(\mathbf{X})$ ,  $\bar{\mathbf{b}} = \text{vec}(\mathbf{B})$ , and  $\bar{\mathbf{A}} = \mathbf{R}_{H1}^T \otimes \mathbf{A}$ , which typically requires operations with a complexity of  $\mathcal{O}((N_t T)^3)$ . Since  $\bar{\mathbf{A}}$  is the Kronecker product of two PSD matrices, it is inherently PSD. Consequently, for any  $\mu > 0$ , the matrix  $\bar{\mathbf{A}} + \mu \mathbf{I}_{N_t T}$  becomes PD, guaranteeing the existence of a unique solution  $\bar{\mathbf{x}} = (\bar{\mathbf{A}} + \mu \mathbf{I}_{N_t T})^{-1} \bar{\mathbf{b}}$ . We refer to this method as FP-KLD and summarize the overall procedure in Algorithm 1.

Beyond the algorithmic description, we present several discussions regarding the proposed FP-KLD to elucidate the theoretical foundations of the algorithm. Specifically, we rigorously analyze its convergence properties by establishing a connection to the MM framework and provide an intuitive interpretation through block coordinate ascent.

**Remark 1** (MM interpretation). We note that the proposed FP-based optimization mechanism also can be understood within the MM framework. Specifically, as shown in Lemma 1, for

any given  $\mathbf{X}$ , introducing the auxiliary variable  $\mathbf{\Gamma} \succeq 0$  produces the surrogate function (23), which serves as a global lower bound of the original objective  $f(\mathbf{X})$ . Crucially, the bound becomes tight at the point  $\mathbf{\Gamma}^*(\mathbf{X}) = (\mathbf{X}\mathbf{L})^H \mathbf{K}_0^{-1} (\mathbf{X}\mathbf{L})$ , which indicates  $\max_{\mathbf{\Gamma}} f_{\ell}(\mathbf{X}, \mathbf{\Gamma}) = f(\mathbf{X})$ . Similar to this, in Lemma 2, we introduce an additional auxiliary variable  $\mathbf{\Psi}$ , the quadratic surrogate (29) is obtained, which is tight at  $\mathbf{\Psi}^*(\mathbf{X}) = \mathbf{K}_1^{-1} \mathbf{X} \mathbf{L}$ . This implies  $\max_{\mathbf{\Psi}} f_q(\mathbf{X}, \mathbf{\Gamma}, \mathbf{\Psi}) = f_{\ell}(\mathbf{X}, \mathbf{\Gamma})$ .

For this reason, the iteration that sets  $\mathbf{\Gamma}^{(t)} = \mathbf{\Gamma}^*(\mathbf{X}^{(t)})$  and  $\mathbf{\Psi}^{(t)} = \mathbf{\Psi}^*(\mathbf{X}^{(t)})$  defines the surrogate

$$g(\mathbf{X} | \mathbf{X}^{(t)}) \triangleq f_q(\mathbf{X}, \mathbf{\Gamma}^{(t)}, \mathbf{\Psi}^{(t)}), \quad (33)$$

which satisfies two key MM properties: (a) it is a global lower bound of the original objective, and (b) it is tight at the current iterate  $\mathbf{X}^{(t)}$ . Consequently, the MM principle guarantees the monotonic improvement

$$f(\mathbf{X}^{(t+1)}) \geq g(\mathbf{X}^{(t+1)} | \mathbf{X}^{(t)}) \geq g(\mathbf{X}^{(t)} | \mathbf{X}^{(t)}) = f(\mathbf{X}^{(t)}). \quad (34)$$

Since the feasible set  $\mathcal{X} = \{\mathbf{X} : \text{Tr}(\mathbf{X}\mathbf{X}^H) \leq P_t\}$  is compact and  $f$  is continuous, the sequence  $\{f(\mathbf{X}^{(t)})\}$  converges to a finite limit, and any accumulation point of  $\mathbf{X}^{(t)}$  is a stationary point of the original problem. We clarify that the connection between matrix FP and MM was well explained in [13].

**Remark 2** (BCA interpretation). The FP iteration can alternatively be interpreted from the perspective of block coordinate ascent (BCA). Define the lifted objective

$$F(\mathbf{X}, \mathbf{\Gamma}, \mathbf{\Psi}) \triangleq f_q(\mathbf{X}, \mathbf{\Gamma}, \mathbf{\Psi}), \quad (35)$$

which by construction satisfies

$$f(\mathbf{X}) = \max_{\mathbf{\Gamma} \succeq 0, \mathbf{\Psi}} F(\mathbf{X}, \mathbf{\Gamma}, \mathbf{\Psi}). \quad (36)$$

In this view, the variables are partitioned into three blocks:  $(\mathbf{\Psi})$ ,  $(\mathbf{\Gamma})$ , and  $(\mathbf{X})$ . Maximizing  $F$  with respect to one block while holding the others fixed yields the following alternating updates:

$$\mathbf{\Gamma}^{(t+1)} = \arg \max_{\mathbf{\Gamma}} F(\mathbf{X}^{(t)}, \mathbf{\Gamma}, \mathbf{\Psi}^{(t)}) = (\mathbf{X}^{(t)} \mathbf{L})^H \mathbf{K}_0^{-1} (\mathbf{X}^{(t)} \mathbf{L}) \quad (37)$$

$$\mathbf{\Psi}^{(t+1)} = \arg \max_{\mathbf{\Psi}} F(\mathbf{X}^{(t)}, \mathbf{\Gamma}^{(t+1)}, \mathbf{\Psi}) = \mathbf{K}_1^{-1} \mathbf{X}^{(t)} \mathbf{L}, \quad (38)$$

$$\mathbf{X}^{(t+1)} = \arg \max_{\mathbf{X} \in \mathcal{X}} F(\mathbf{X}, \mathbf{\Gamma}^{(t+1)}, \mathbf{\Psi}^{(t+1)}), \quad (39)$$

From the above update processes, two observations follow. First, the updates for  $\mathbf{\Gamma}$  and  $\mathbf{\Psi}$  admit closed-form solutions, which can be computed efficiently at each iteration. Second, the  $\mathbf{X}$ -update reduces to a structured convex or quadratic optimization problem, for which efficient numerical solvers or even analytic updates may be available. Because each block is optimized exactly, the lifted objective  $F$  is monotonically non-decreasing across iterations. Furthermore, since  $F$  is a tight reformulation of  $f$ , the monotonicity of  $F$  directly implies monotonicity of the original KLD objective  $f$ .

For this reason, the FP can be equivalently viewed as a BCA (or alternating maximization) method applied to the augmented problem. This perspective not only highlights the intuitive coordinate-wise optimization structure of the algorithm, but also guarantees convergence of the proposed method by standard results on BCA under mild regularity conditions.

#### IV. ACCELERATED MM-BASED KLD OPTIMIZATION

In the previous section, we develop a tractable iterative algorithm to solve a generic KLD optimization problem. Nonetheless, its final subproblem, as shown in (32), requires solving a large-scale linear system at each iteration. This step, originating from the matrix inversion embedded in the quadratic transform, incurs a high computational complexity of order  $\mathcal{O}((N_t T)^3)$ , which can be prohibitive in practice. To resolve this issue, we present reduced-complexity FP-KLD variants in this section, referred to as MM-KLD and A-MM-KLD. The two key ideas underlying these methods are as follows. First, to eliminate the costly subproblem, we apply a *nonhomogeneous relaxation* technique to the concave quadratic surrogate  $f_q$ . This relaxation replaces the complex, anisotropic curvature of the subproblem, i.e., the term  $\bar{\mathbf{x}}^H \bar{\mathbf{A}} \bar{\mathbf{x}}$ , with a simple isotropic spectral bound of the form  $\lambda \|\bar{\mathbf{x}}\|^2$ , yielding an update for  $\mathbf{X}$  in a simple, closed form.

However, this computational gain comes at the cost of an increased number of iterations required for convergence. This is because the nonhomogeneous bound is inherently looser than the original quadratic surrogate, causing the algorithm to take more conservative steps and thus increasing the total number of iterations. To counteract this, our second key idea is to employ acceleration techniques. By interpreting the iterative algorithm as a fixed-point mapping, we apply acceleration techniques such as the *STEM* method to substantially reduce the number of iterations, resulting in a computationally light and fast-converging algorithm [37].

##### A. Nonhomogeneous Relaxation

Algorithm 1 provides a direct method for solving the  $\mathbf{X}$ -subproblem by analyzing the KKT conditions. In this section, we present an approach that further simplifies the subproblem to yield an update for  $\mathbf{X}$  in a closed-form expression, avoiding the need to solve a complicated linear system and to compute a matrix inversion.

To achieve this, we focus on the vectorized quadratic term within the objective function. As previously shown, the parts of  $f_q$  involving  $\mathbf{X}$  can be written as:

$$\begin{aligned} & 2 \Re \{ \text{Tr}(\mathbf{\Gamma} \mathbf{\Psi}^H \mathbf{X} \mathbf{L}) \} - \text{Tr}(\mathbf{X} \mathbf{R}_{H1} \mathbf{X}^H \mathbf{\Psi} \mathbf{\Gamma} \mathbf{\Psi}^H) \\ &= \text{Tr}(2 \Re \{ (\mathbf{X} \mathbf{L})^H \mathbf{\Psi} \mathbf{\Gamma} \}) - \text{Tr}(\mathbf{X} \mathbf{R}_{H1} \mathbf{X}^H \mathbf{A}) \\ &= 2 \Re \{ \bar{\mathbf{x}}^H \bar{\mathbf{b}} \} - \bar{\mathbf{x}}^H \bar{\mathbf{A}} \bar{\mathbf{x}}, \end{aligned} \quad (40)$$

where  $\bar{\mathbf{x}} = \text{vec}(\mathbf{X})$ . The core of this alternative approach lies in constructing a simpler surrogate for the quadratic term  $\bar{\mathbf{x}}^H \bar{\mathbf{A}} \bar{\mathbf{x}}$  by applying a nonhomogeneous relaxation. The key to this relaxation is the following lemma.

**Lemma 3** (Nonhomogeneous bound [38]). *Consider two Hermitian matrices  $\mathbf{P}$  and  $\mathbf{K}$  such that  $\mathbf{P} \prec \mathbf{K}$ . Then, for any  $\mathbf{x}$  and  $\mathbf{z}$ ,*

$$\mathbf{x}^H \mathbf{P} \mathbf{x} \leq \mathbf{x}^H \mathbf{K} \mathbf{x} + 2 \Re \{ \mathbf{x}^H (\mathbf{P} - \mathbf{K}) \mathbf{z} \} + \mathbf{z}^H (\mathbf{K} - \mathbf{P}) \mathbf{z}, \quad (41)$$

with equality if and only if  $\mathbf{z} = \mathbf{x}$ .

*Proof sketch.* Since  $\mathbf{K} - \mathbf{P} \succ \mathbf{0}$ ,  $\mathbf{v}^H (\mathbf{K} - \mathbf{P}) \mathbf{v} \geq 0$  for any  $\mathbf{v}$ . Let  $\mathbf{v}$  as  $\mathbf{z} - \mathbf{x}$ , then

$$\begin{aligned} \mathbf{v}^H (\mathbf{K} - \mathbf{P}) \mathbf{v} &= (\mathbf{z} - \mathbf{x})^H (\mathbf{K} - \mathbf{P}) (\mathbf{z} - \mathbf{x}) \\ &= \mathbf{z}^H (\mathbf{K} - \mathbf{P}) \mathbf{z} - 2 \Re \{ \mathbf{x}^H (\mathbf{K} - \mathbf{P}) \mathbf{z} \} \\ &\quad + \mathbf{x}^H \mathbf{K} \mathbf{x} - \mathbf{x}^H \mathbf{P} \mathbf{x} \geq 0 \end{aligned} \quad (42)$$

Thus, (41) holds for any  $\mathbf{x}$  and  $\mathbf{z}$ . The equality holds if and only if  $\mathbf{z} = \mathbf{x}$ . ■

Applying Lemma 3 to the quadratic term  $\bar{\mathbf{x}}^H \bar{\mathbf{A}} \bar{\mathbf{x}}$  with  $\mathbf{P} = \bar{\mathbf{A}}$  and  $\mathbf{K} = \bar{\lambda} \mathbf{I}_{N_t T}$ , where  $\lambda_p$  is the largest eigenvalue of  $\bar{\mathbf{A}}$  and  $\bar{\lambda} \triangleq \lambda_p + \delta$  for a small  $\delta > 0$  (so that  $\bar{\mathbf{A}} \prec \bar{\lambda} \mathbf{I}_{N_t T}$ ), we introduce an auxiliary variable  $\bar{\mathbf{z}} \in \mathbb{C}^{N_t T}$  and derive the surrogate

$$\begin{aligned} & \underset{\mathbf{X}, \mathbf{\Gamma}, \mathbf{\Psi}, \bar{\mathbf{z}}}{\text{maximize}} \quad f_h(\bar{\mathbf{x}}, \mathbf{\Gamma}, \mathbf{\Psi}, \bar{\mathbf{z}}) \\ & \text{subject to} \quad \|\bar{\mathbf{x}}\|^2 \leq P_t, \quad \bar{\mathbf{x}} = \text{vec}(\mathbf{X}) \end{aligned} \quad (43)$$

with

$$\begin{aligned} f_h(\bar{\mathbf{x}}, \mathbf{\Gamma}, \mathbf{\Psi}, \bar{\mathbf{z}}) &= \log |\mathbf{I}_{N_t} + \mathbf{\Gamma}| - \text{Tr}(\mathbf{\Gamma}) - \text{Tr}(\mathbf{R}_N \mathbf{A}) + 2 \Re \{ \bar{\mathbf{x}}^H \bar{\mathbf{b}} \} \\ &\quad + 2 \Re \{ \bar{\mathbf{x}}^H (\bar{\lambda} \mathbf{I}_{N_t T} - \bar{\mathbf{A}}) \bar{\mathbf{z}} \} + \bar{\mathbf{z}}^H (\bar{\mathbf{A}} - \bar{\lambda} \mathbf{I}_{N_t T}) \bar{\mathbf{z}} \\ &\quad - \bar{\lambda} \bar{\mathbf{x}}^H \bar{\mathbf{x}}. \end{aligned} \quad (44)$$

Given  $\mathbf{X}$  (or equivalently  $\bar{\mathbf{x}}$ ), by the equality condition of Lemma 3, the optimal value of the new auxiliary variable simply follows as

$$\bar{\mathbf{z}}^* = \bar{\mathbf{x}} \quad (45)$$

Subsequently, for fixed  $\{\mathbf{\Gamma}, \mathbf{\Psi}, \bar{\mathbf{z}}\}$  at current iteration, we update  $\bar{\mathbf{x}}$  by maximizing the objective  $f_h$  of (44). Since  $f_h$  is a concave quadratic function with respect to  $\bar{\mathbf{x}}$ , its unconstrained maximizer is found by setting the gradient with respect to  $\bar{\mathbf{x}}$  to zero:

$$2(\bar{\mathbf{b}} + (\bar{\lambda} \mathbf{I}_{N_t T} - \bar{\mathbf{A}}) \bar{\mathbf{z}} - \bar{\lambda} \bar{\mathbf{x}}) = \mathbf{0} \quad (46)$$

The final update for  $\bar{\mathbf{x}}^*$  is obtained by projecting this unconstrained solution onto the feasible set defined by the power constraint, which results in the closed form expression:

$$\bar{\mathbf{x}}^* = \sqrt{P_t} \frac{\bar{\mathbf{b}} + (\bar{\lambda} \mathbf{I}_{N_t T} - \bar{\mathbf{A}}) \bar{\mathbf{z}}}{\|\bar{\mathbf{b}} + (\bar{\lambda} \mathbf{I}_{N_t T} - \bar{\mathbf{A}}) \bar{\mathbf{z}}\|}. \quad (47)$$

Based on these derived update rules, the overall optimization strategy is established. This three-stage framework—dual, quadratic, and nonhomogeneous transforms—yields a sequence of convex subproblems in  $\mathbf{X}$  that can be solved efficiently until convergence. Specifically, the inclusion of the final nonhomogeneous transform replaces the direct solution of a linear system, which has a complexity of  $\mathcal{O}((N_t T)^3)$ , with a simple closed-form update. The dominant cost is computing the spectral radius  $\bar{\lambda}$  via  $k$  power iterations, requiring only  $\mathcal{O}(k(N_t T)^2)$ , where  $k$  is typically a small number [39], [40]. The complete iterative procedure incorporating the nonhomogeneous relaxation is formally summarized in Algorithm 2, which we refer to as MM-KLD.

We now justify the convergence of the proposed MM-KLD by showing it adheres to the MM principle. The nonhomogeneous relaxation introduces a second level of minorization.

---

**Algorithm 2:** MM-KLD

---

```

1 Input:  $P_t$ ,  $\epsilon > 0$ ,  $t_{\max}$ ,  $\delta > 0$ ,  $\mathbf{R}_{H1}$ ,  $\mathbf{R}_0$ ,  $\mathbf{R}_N$ , and  $\mathbf{X}_{\text{init}}$ 
2 Precompute:  $\mathbf{R}_{H1} - \mathbf{R}_0 = \mathbf{L}\mathbf{L}^H$ 
3 Initialize:  $\mathbf{X}^{(0)} \leftarrow \mathbf{X}_{\text{init}}$ ; set  $t \leftarrow 0$ 
4 while  $t < t_{\max}$  do
5   Compute  $\mathbf{K}_0$  by (6) and  $\mathbf{K}_1$  by (7)
6   Update  $\mathbf{\Gamma}^{(t+1)}$  by (24).
7   Update  $\mathbf{\Psi}^{(t+1)}$  by (30).
8   Update  $\bar{\mathbf{z}}^{(t+1)}$  by (45)
9   Update  $\mathbf{X}^{(t+1)}$  by solving (47) and reshaping  $\bar{\mathbf{x}}$ .
10  if  $\frac{f(\mathbf{X}^{(t+1)}) - f(\mathbf{X}^{(t)})}{f(\mathbf{X}^{(t)})} < \epsilon$  then
11    break
12  end
13   $t \leftarrow t + 1$ 
14 end
15 Output:  $\mathbf{X}^* \leftarrow \mathbf{X}^{(t+1)}$ .

```

---

We define a new surrogate function for the relaxed algorithm as

$$h(\mathbf{X}|\mathbf{X}^{(t)}) \triangleq f_h(\bar{\mathbf{x}}, \mathbf{\Gamma}^{(t+1)}, \mathbf{\Psi}^{(t+1)}, \bar{\mathbf{z}}^{(t+1)}), \quad (48)$$

where all the auxiliary variables  $\mathbf{\Gamma}^{(t+1)}, \mathbf{\Psi}^{(t+1)}, \bar{\mathbf{z}}^{(t+1)}$  are updated based on  $\mathbf{X}^{(t)}$ .

This new surrogate  $h(\mathbf{X}|\mathbf{X}^{(t)})$  satisfies the two key properties of an MM algorithm. First, by construction,  $f_h$  is a global lower bound of  $f_q$  (Lemma 3), and  $f_q$  is a global lower bound of  $f$ , which by transitivity makes  $h(\mathbf{X}|\mathbf{X}^{(t)})$  a global lower bound of  $f(\mathbf{X})$ . Second, at the current iterate  $\mathbf{X}^{(t)}$ , all auxiliary variables are chosen precisely to meet the equality conditions of their respective transformations. These choices for  $\mathbf{\Gamma}$  and  $\mathbf{\Psi}$  ensure the tightness of the first-level surrogate  $g$  as shown in Remark 1, while the choice  $\bar{\mathbf{z}}^{(t+1)} = \bar{\mathbf{x}}^{(t)}$  ensures the tightness of the second-level surrogate  $h$ .

Maximizing this tight surrogate yields the update  $\mathbf{X}^{(t+1)}$ , leading to the standard ascent inequality, analogous to (34):

$$f(\mathbf{X}^{(t+1)}) \geq h(\mathbf{X}^{(t+1)}|\mathbf{X}^{(t)}) \geq h(\mathbf{X}^{(t)}|\mathbf{X}^{(t)}) = f(\mathbf{X}^{(t)}). \quad (49)$$

Thus, the inequality chain (49) guarantees a monotonic ascent for the original objective  $f(\mathbf{X})$ . This confirms that Algorithm 2 is also a valid instantiation of the MM algorithm.

Although the nonhomogeneous relaxation is tight at the current iterate  $\mathbf{X}^{(t)}$ , (44) replaces the anisotropic curvature  $\bar{\mathbf{x}}^H \bar{\mathbf{A}} \bar{\mathbf{x}}$  with an isotropic spectral bound  $\bar{\lambda} \bar{\mathbf{x}}^H \bar{\mathbf{x}}$  along with corresponding linear terms, leading to a more conservative step. Therefore, FP-KLD produces a steeper ascent per iteration than the nonhomogeneous variant, whereas in terms of runtime, the nonhomogeneous method is significantly faster due to its much lower per-iteration cost.

**Remark 3** (Comparison with the MM baseline in [21]). It is instructive to compare our proposed framework with the benchmark MM algorithm in [21] regarding the construction of the surrogate function. The benchmark method adopts a piecewise decomposition approach: it splits the intricate KLD objective into three separate log-det and trace terms, and

then employs first-order Taylor expansions (i.e., supporting hyperplane) to bound the convex parts based on local gradient information. The final quadratic surrogate is then formed by summing these local approximations.

In contrast, our FP-based approach reformulates the objective globally using auxiliary variables. Instead of relying on gradient-based linearizations, we apply a sequence of matrix FP to fundamentally alter the algebraic structure of the problem. This procedure effectively decouples the matrix inverses from the design variables within the log-det and trace-ratio terms, naturally yielding a quadratic surrogate.

Crucially, this difference leads to a significant advantage in computational efficiency. In the benchmark method, updating the waveform requires solving a linear system at every iteration, which imposes a complexity of  $\mathcal{O}(n^3)$ , where  $n$  denotes the dimension of the optimization variable. Our approach overcomes this bottleneck by incorporating the nonhomogeneous relaxation into the FP-derived quadratic surrogate. By replacing the complex anisotropic curvature with a simple isotropic spectral bound, we obtain a closed-form update that avoids solving any large-scale linear system, thereby drastically reducing the per-iteration complexity to  $\mathcal{O}(kn^2)$  required for the power iterations.

### B. Acceleration

In the previous subsection, we introduced the nonhomogeneous relaxation (Algorithm 2) to reduce the high per-iteration cost of the original FP-KLD algorithm. This computational gain, however, stems from using the isotropic surrogate  $f_h$ , which is inherently looser than the anisotropic quadratic surrogate  $f_q$ . Consequently, while each step is much faster, the algorithm typically requires a larger total number of iterations to reach the same solution. To compensate for this trade-off, we use an acceleration technique.

To motivate the use of acceleration schemes, it is essential to interpret our optimization framework as a fixed-point mapping. At iteration  $t$ , the auxiliary variables  $\mathbf{\Gamma}^{(t)}$ ,  $\mathbf{\Psi}^{(t)}$ , and the vectorized auxiliary  $\bar{\mathbf{z}}^{(t)}$  are updated in closed form based on the current  $\mathbf{X}^{(t)}$ . Subsequently, the next iterate,  $\mathbf{X}^{(t+1)}$ , is obtained by maximizing the resulting surrogate objective, which is now parameterized by these fixed auxiliary variables. This leads to the following remark.

**Remark 4** (Fixed-point iteration interpretation). The two-stage procedure, where the auxiliary variables are first determined by  $\mathbf{X}^{(t)}$  and then in turn determine  $\mathbf{X}^{(t+1)}$ , can be encapsulated by a single nonlinear mapping operator,  $\mathcal{M}(\cdot)$ . This allows the entire update rule to be expressed concisely as a fixed-point iteration:

$$\mathbf{X}^{(t+1)} = \mathcal{M}(\mathbf{X}^{(t)}) \quad (50)$$

The algorithm's goal is thus to find the fixed point  $\mathbf{X}^*$  that satisfies  $\mathbf{X}^* = \mathcal{M}(\mathbf{X}^*)$ . This interpretation is particularly valuable because algorithms derived from the MM principle, while guaranteeing monotonic convergence, often exhibit a slow, linear convergence rate if the problem is ill-conditioned [41], [42]. This slow convergence can make achieving a high-precision solution prohibitively time-consuming. By framing

our method as a fixed-point iteration, we can directly leverage a suite of well-established acceleration schemes designed for general fixed-point iterations to enhance practical performance.

Applying acceleration modifies the update step of MM-KLD. Instead of simply setting  $\mathbf{X}^{(t+1)} = \mathcal{M}(\mathbf{X}^{(t)})$ , we use the unaccelerated output  $\mathcal{M}(\mathbf{X}^{(t)})$  as an input to an acceleration formula, which then computes the final  $\mathbf{X}^{(t+1)}$  for the next iterate.

While various well-established acceleration schemes exist, such as Polyak's heavy-ball [43] and Nesterov acceleration [44], we focus on a Steffensen-type method (STEM) [37] for our framework. STEM is a modern vector generalization of the classical scalar Steffensen's method [45], [46], designed to accelerate general fixed-point iterations. This method is an effective derivative-free technique that requires only the fixed-point mapping  $\mathcal{M}(\cdot)$  itself, yet it constructs a secant approximation that achieves a quadratic convergence rate near the solution, offering a substantial speed-up over the linear convergence of the baseline MM algorithm [41].

The core of STEM is to define a residual function:

$$\mathbf{R}(\mathbf{X}) = \mathcal{M}(\mathbf{X}) - \mathbf{X}, \quad (51)$$

and, at iteration  $t$ , compute the two successive images

$$\Theta_1 = \mathcal{M}(\mathbf{X}^{(t)}), \quad (52)$$

$$\Theta_2 = \mathcal{M}(\Theta_1). \quad (53)$$

Let the first residual and the second one be

$$\Delta_t = \Theta_1 - \mathbf{X}^{(t)} = \mathbf{R}(\mathbf{X}^{(t)}) \quad (54)$$

$$\mathbf{W}_t = \Theta_2 - 2\Theta_1 + \mathbf{X}^{(t)} = \mathbf{R}(\Theta_1) - \mathbf{R}(\mathbf{X}^{(t)}) \quad (55)$$

The accelerated candidate is taken along the residual direction with a step size  $\gamma_t$  as

$$\gamma_t = \frac{\langle \Delta_t, \Delta_t \rangle}{\langle \Delta_t, \mathbf{W}_t \rangle} \quad (56)$$

$$\mathbf{X}_{\text{cand}}^{(t+1)} = \mathbf{X}^{(t)} - \gamma_t \Delta_t \quad (57)$$

$$\mathbf{X}^{(t+1)} = \mathcal{P}(\mathbf{X}_{\text{cand}}^{(t+1)}) \quad (58)$$

Here  $\mathcal{P}(\cdot)$  is the projection operator that maps a candidate solution back onto the constraint feasible set. Intuitively,  $\gamma_t$  is chosen so that the next residual is orthogonal to the current residual under a local secant approximation, thereby removing the leading error component.

Because STEM steps do not inherently guarantee the non-decreasing property, we employ a simple monotonicity check with backtracking: if the objective fails to increase, we shrink the step length via  $\gamma_t \leftarrow (\gamma_t - 1)/2$ , recompute the candidate, and repeat until acceptance. As this rule is iterated,  $\gamma_t \rightarrow -1$ , in which case the update falls back to  $\mathbf{X}^{(t)} - \gamma_t \Delta_t = \Theta_1 = \mathcal{M}(\mathbf{X}^{(t)})$ , which is exactly the baseline MM step. This mechanism ensures that the algorithm preserves the monotonicity guaranteed by the original MM framework.

**Remark 5** (Why Steffensen-type acceleration?). While momentum-based methods like Polyak's and Nesterov's are powerful, they are fundamentally first-order schemes. That

---

### Algorithm 3: A-MM-KLD

---

```

1 Input:  $P_t$ ,  $\epsilon > 0$ ,  $t_{\max}$ ,  $\delta > 0$ ,  $\mathbf{R}_{H1}, \mathbf{R}_0, \mathbf{R}_N$ , and  $\mathbf{X}_{\text{init}}$ 
2 Precompute:  $\mathbf{R}_{H1} - \mathbf{R}_0 = \mathbf{L}\mathbf{L}^H$ 
3 Initialize:  $\mathbf{X}^{(0)} \leftarrow \mathbf{X}_{\text{init}}$ ; set  $t \leftarrow 0$ 
4 while  $t < t_{\max}$  do
5   Compute  $\mathbf{K}_0$  by (6) and  $\mathbf{K}_1$  by (7)
6   Compute  $\mathcal{M}(\mathbf{X}^{(t)})$ ,  $\mathcal{M}(\Theta_1)$  using (24), (30), (45) and solving (47) followed by reshaping.
7   Compute the residuals  $\Delta_t, \mathbf{W}_t$  by (54), (55).
8   Compute the step size  $\gamma_t$  by (56).
9   repeat
10     $\mathbf{X}_{\text{cand}}^{(t+1)} \leftarrow \mathbf{X}^{(t)} - \gamma_t \Delta_t$ 
11     $\mathbf{X}^{(t+1)} \leftarrow \sqrt{P_t} \frac{\mathbf{X}_{\text{cand}}^{(t+1)}}{\|\mathbf{X}_{\text{cand}}^{(t+1)}\|_F}$ 
12    if  $f(\mathbf{X}^{(t+1)}) < f(\mathbf{X}^{(t)})$  then
13       $\gamma_t \leftarrow (\gamma_t - 1)/2$ 
14    end
15    until  $f(\mathbf{X}^{(t+1)}) \geq f(\mathbf{X}^{(t)})$ ;
16    if  $\frac{f(\mathbf{X}^{(t+1)}) - f(\mathbf{X}^{(t)})}{f(\mathbf{X}^{(t)})} < \epsilon$  then
17      break
18    end
19     $t \leftarrow t + 1$ 
20 end
21 Output:  $\mathbf{X}^* \leftarrow \mathbf{X}^{(t+1)}$ .

```

---

is to say, they operate by blending the previous step's direction, i.e., momentum, with the current map's output. This helps dampen oscillations and improves the constant of linear convergence, but it does not elevate the fundamental order of convergence, which remains linear.

STEM is a fundamentally different and more sophisticated approach, acting as a derivative-free analogue to the quadratically convergent Newton's method. Instead of relying on history, it actively probes the local geometry of the map  $\mathcal{M}(\cdot)$  by computing two successive images. As shown in (55), the difference  $\mathbf{W}_t$  implicitly captures information about the map's local derivative, i.e., its Jacobian. STEM uses this information to build a secant model and take an approximate Newton step, achieving a quadratic convergence rate.

This makes it a synergistic choice for our framework. The primary cost of STEM is the second map evaluation. However, we have just demonstrated the MM-KLD, whose entire purpose was to make the single iterate computationally cheap by avoiding the linear system solve of size  $N_t T$ .

Algorithm 3 formalizes this procedure, integrating the computationally efficient map from Algorithm 2 with the STEM's acceleration steps. We name this complete framework A-MM-KLD. This approach combines the low per-iteration cost of the nonhomogeneous relaxation with the fast quadratic convergence of STEM, resulting in a highly efficient and robust algorithm for KLD maximization.

## V. EXTENSIONS AND APPLICATION SCENARIOS

In this section, we demonstrate the versatility of the proposed optimization framework. We first show that the proposed FP-KLD can be seamlessly extended to the joint waveform design in ISAC systems. Subsequently, we apply the framework to a multiple random access scenario to maximize activity detection reliability.

### A. Joint Waveform Design for ISAC

The proposed FP-KLD, originally developed for KLD maximization in sensing, can be directly extended to joint waveform design in ISAC systems. This subsection explains its applicability to ISAC waveform design.

A primary objective in ISAC is to optimize a joint utility function that jointly accounts for sensing and communication performance metrics. One possible formulation is a weighted sum of KLD (as a sensing performance metric) and the MI (as a communication performance metric), given by:

$$\begin{aligned} & \underset{\mathbf{X}}{\text{maximize}} \quad (1 - \rho) D_{\text{KL}}(\mathbf{Y}_0 \parallel \mathbf{Y}_1) + \rho I(\mathbf{X}; \mathbf{Y}_c), \\ & \text{subject to} \quad \text{Tr}(\mathbf{X}\mathbf{X}^H) \leq P_t, \end{aligned} \quad (59)$$

where  $\mathbf{Y}_c = \mathbf{H}_c \mathbf{X}^H + \mathbf{N}_c$ . Here,  $\mathbf{Y}_c$ ,  $\mathbf{H}_c$ , and  $\mathbf{N}_c$  denote the received signal, channel matrix, and zero-mean Gaussian noise with covariance  $\mathbf{R}_{n,c}$ , respectively. This formulation corresponds to a standard approach for characterizing the fundamental trade-off between sensing and communication, consistent with recent ISAC frameworks [4], [5], [47]. As such, it provides a unified performance metric for joint waveform design. As discussed in the earlier section, a significant challenge in solving (59) lies in the disparity among the available optimization tools. Our proposed FP-KLD directly addresses this bottleneck by providing a computationally tractable surrogate for the KLD. Specifically, as FP is a well-established tool for MI maximization in communication systems, our approach renders the ISAC optimization problem amenable to FP; resulting in that the composite ISAC objective function is efficiently handled by applying the same FP principles [7], [13], [26].

Now we explain the detailed mechanism for joint ISAC waveform design using FP. By applying the determinant lemma [33], the MI is given by

$$\begin{aligned} I(\mathbf{X}; \mathbf{Y}_c) &= \log |\mathbf{I} + \mathbf{R}_{n,c}^{-1} \mathbf{H}_c \mathbf{X} \mathbf{X}^H \mathbf{H}_c^H| \\ &= \log |\mathbf{I} + (\mathbf{H}_c \mathbf{X})^H \mathbf{R}_{n,c}^{-1} \mathbf{H}_c \mathbf{X}| \end{aligned} \quad (60)$$

To unify this with the KLD optimization, we apply the proposed sequence of transforms introducing two auxiliary variables, as in FP-KLD. First, Lemma 1 with an auxiliary variable  $\mathbf{\Gamma}_c \succeq \mathbf{0}$  yields a lower bound

$$\begin{aligned} f_{c,l}(\mathbf{X}, \mathbf{\Gamma}_c) &= \log |\mathbf{I} + \mathbf{\Gamma}_c| - \text{Tr}(\mathbf{\Gamma}_c) + \text{Tr}((\mathbf{I} + \mathbf{\Gamma}_c) \cdot \\ & \quad (\mathbf{H}_c \mathbf{X})^H (\mathbf{H}_c \mathbf{X} \mathbf{X}^H \mathbf{H}_c^H + \mathbf{R}_{n,c})^{-1} (\mathbf{H}_c \mathbf{X})). \end{aligned} \quad (61)$$

Subsequently, applying Lemma 2 with an auxiliary variable  $\mathbf{\Psi}_c$  results in the final surrogate as:

$$\begin{aligned} f_{c,q}(\mathbf{X}, \mathbf{\Gamma}_c, \mathbf{\Psi}_c) &= \log |\mathbf{I} + \mathbf{\Gamma}_c| - \text{Tr}(\mathbf{\Gamma}_c) + \text{Tr}((\mathbf{I} + \mathbf{\Gamma}_c) \cdot \\ & \quad (2\Re\{(\mathbf{H}_c \mathbf{X})^H \mathbf{\Psi}_c\} - \mathbf{\Psi}_c^H (\mathbf{H}_c \mathbf{X} \mathbf{X}^H \mathbf{H}_c^H + \mathbf{R}_{n,c}) \mathbf{\Psi}_c)) \\ &= \text{const.} + 2\Re\{\text{Tr}((\mathbf{I} + \mathbf{\Gamma}_c) \mathbf{\Psi}_c^H \mathbf{H}_c \mathbf{X})\} \\ & \quad - \text{Tr}(\mathbf{X}^H \mathbf{H}_c^H \mathbf{\Psi}_c (\mathbf{I} + \mathbf{\Gamma}_c) \mathbf{\Psi}_c^H \mathbf{H}_c \mathbf{X}), \end{aligned} \quad (62)$$

where *const.* denotes the terms independent of  $\mathbf{X}$ . Since  $f_{c,q}$  is a concave quadratic function of  $\mathbf{X}$ , sharing the exact algebraic structure as in (29), the joint ISAC problem (59) is efficiently solved by iteratively maximizing the global surrogate  $(1 - \rho)f_q + \rho f_{c,q}$ . This involves updating the auxiliary variables  $\mathbf{\Gamma}$ ,  $\mathbf{\Psi}$ ,  $\mathbf{\Gamma}_c$ ,  $\mathbf{\Psi}_c$ , followed by a unified quadratic update for  $\mathbf{X}$ . This highlights a seamless extension of the proposed FP-KLD method to joint waveform optimization in ISAC systems.

### B. Multiple Random Access

In this subsection, we present another application scenario for the proposed optimization technique. To be specific, we consider a multiple random access problem, which aims to design a random access waveform that maximizes the reliability of activity detection.

In typical cellular networks, random access is handled by assigning quasi-orthogonal sequences (e.g., Zadoff-Chu [48], [49]) to devices, which simplifies detection. However, the performance of such fixed sequences degrades severely in the presence of strong multi-user interference (MUI) or in non-orthogonal settings that may arise from an increasing number of users. To resolve this, we instead formulate the problem as maximizing the sum of KLD between the active and inactive hypotheses for all users, averaged over the activity patterns of interfering devices. This approach allows us to jointly optimize the waveforms to be robust to MUI, offering a significant advantage over fixed-sequence designs.

1) *Model and Problem Formulation:* We consider a random access setting with  $K$  devices. Over  $T$  snapshots, the received signal  $\mathbf{Y} \in \mathbb{C}^{T \times N_r}$  is

$$\mathbf{Y} = \sum_{i=1}^K \mathbf{X}_i \mathbf{H}_i + \mathbf{N}, \quad (63)$$

where  $\mathbf{X}_i \in \mathbb{C}^{T \times N_r}$  is the waveform of device  $i$ . The columns of  $\mathbf{H}_i \in \mathbb{C}^{N_r \times N_r}$  are i.i.d., each distributed as  $\mathcal{CN}(\mathbf{0}, \mathbf{R}_i)$ . Thus, the covariance matrix of  $\text{vec}(\mathbf{H}_i)$  is  $\mathbf{I}_{N_r} \otimes \mathbf{R}_i$ . The noise  $\mathbf{N}$  is zero-mean complex Gaussian with independent columns, each with covariance  $\mathbf{R}_N$ ; hence, the covariance matrix of  $\text{vec}(\mathbf{N})$  is equal to  $\mathbf{I}_{N_r} \otimes \mathbf{R}_N$ .

For each device  $i$ , we test in parallel

$$\begin{aligned} \mathcal{H}_0^{(i)} &: \text{device } i \text{ is inactive} \\ \mathcal{H}_1^{(i)} &: \text{device } i \text{ is active.} \end{aligned}$$

Let  $\mathbf{s}_{-i} \in \{0, 1\}^{K-1}$  denote the on/off activity pattern of the interfering devices (i.e., all devices except device  $i$ ), and let  $\mathcal{S}_{-i}$  be the set of all such patterns. We assume the per-user

activity priors  $\{p_j\}_{j=1}^K$  are known and independent across devices. Then the probability mass function of  $\mathbf{s}_{-i}$  is

$$w(\mathbf{s}_{-i}) = \prod_{j \neq i} p_j^{s_j} (1 - p_j)^{1-s_j}, \quad \mathbf{s}_{-i} \in \mathcal{S}_{-i}, \quad (64)$$

where  $s_j$  is the element of  $\mathbf{s}_{-i}$  corresponding to device  $j$ . Crucially, the distribution of the interference pattern  $\mathbf{s}_{-i}$  is independent of the hypothesis tested for device  $i$ . Conditioned on  $\mathbf{s}_{-i}$ , the observation is complex Gaussian with zero-mean and covariance matrices

$$\mathbf{K}_{i,0}(\mathbf{s}_{-i}) = \mathbf{R}_N + \sum_{j \neq i} s_j \mathbf{X}_j \mathbf{R}_j \mathbf{X}_j^H, \quad (65)$$

$$\mathbf{K}_{i,1}(\mathbf{s}_{-i}) = \mathbf{K}_{i,0}(\mathbf{s}_{-i}) + \mathbf{X}_i \mathbf{R}_i \mathbf{X}_i^H. \quad (66)$$

2) *Design Objective and FP-KLD Instantiation*: Define the joint distributions over the latent interference state and the snapshots:

$$P_{i,0}(\mathbf{s}_{-i}, \mathbf{Y}) = w(\mathbf{s}_{-i}) p_{\mathcal{CN}}(\bar{\mathbf{y}}; \mathbf{I}_{N_r} \otimes \mathbf{K}_{i,0}(\mathbf{s}_{-i})), \quad (67)$$

$$P_{i,1}(\mathbf{s}_{-i}, \mathbf{Y}) = w(\mathbf{s}_{-i}) p_{\mathcal{CN}}(\bar{\mathbf{y}}; \mathbf{I}_{N_r} \otimes \mathbf{K}_{i,1}(\mathbf{s}_{-i})), \quad (68)$$

where  $\bar{\mathbf{y}} = \text{vec}(\mathbf{Y})$ . Since the prior  $w(\mathbf{s}_{-i})$  is common to both hypotheses, the chain rule gives

$$\begin{aligned} & D_{\text{KL}}(P_{i,0}(\mathbf{s}_{-i}, \mathbf{Y}) \| P_{i,1}(\mathbf{s}_{-i}, \mathbf{Y})) \\ &= \mathbb{E}_{\mathbf{s}_{-i} \sim w} \left[ D_{\text{KL}}(p_{\mathcal{CN}}(\bar{\mathbf{y}}; \mathbf{I}_{N_r} \otimes \mathbf{K}_{i,0}(\mathbf{s}_{-i})) \right. \\ & \quad \left. \| p_{\mathcal{CN}}(\bar{\mathbf{y}}; \mathbf{I}_{N_r} \otimes \mathbf{K}_{i,1}(\mathbf{s}_{-i})) \right]. \end{aligned} \quad (69)$$

Therefore, the joint error exponent for user  $i$  equals a weighted sum of Gaussian KLDs. Summing over users yields the multi-user design objective to be maximized as:

$$\begin{aligned} D_{\Sigma}(\{\mathbf{X}_i\}) &\triangleq \sum_{i=1}^K D_{\text{KL}}(P_{i,0} \| P_{i,1}) \\ &= N_r \sum_{i=1}^K \sum_{\mathbf{s}_{-i} \in \mathcal{S}_{-i}} w(\mathbf{s}_{-i}) \left( \log |\mathbf{K}_{i,1}(\mathbf{s}_{-i}) \mathbf{K}_{i,0}^{-1}(\mathbf{s}_{-i})| \right. \\ & \quad \left. + \text{Tr}(\mathbf{K}_{i,1}^{-1}(\mathbf{s}_{-i}) \mathbf{K}_{i,0}(\mathbf{s}_{-i})) - T \right). \end{aligned} \quad (70)$$

We maximize (70) subject to per-device power constraints  $\text{Tr}(\mathbf{X}_i \mathbf{X}_i^H) \leq P_t$ . Finally, the optimization problem formulation follows as:

$$\begin{aligned} & \underset{\{\mathbf{X}_i\}_{i=1}^K}{\text{maximize}} \quad D_{\Sigma}(\{\mathbf{X}_i\}) \\ & \text{subject to} \quad \text{Tr}(\mathbf{X}_i \mathbf{X}_i^H) \leq P_t, \quad \text{for } i = 1, \dots, K. \end{aligned} \quad (71)$$

Since each term in (71) has the same algebraic form as in the single-Gaussian case, our algorithms introduced in previous sections (e.g., FP-KLD and A-MM-KLD) are suitably applied. In the next section, we show that the waveforms optimized via our A-MM-KLD significantly outperform traditional designs in terms of detection probability.

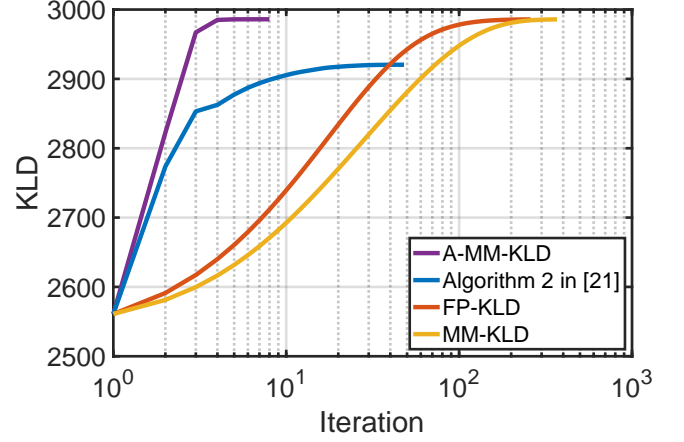


Fig. 1: Convergence profile of the objective function versus the number of iterations. The proposed algorithms are compared with the benchmark method in [21].

## VI. NUMERICAL RESULTS

In this section, we evaluate the performance of the proposed FP-based optimization methods via numerical simulations. We validate the effectiveness of our approach in two distinct scenarios: 1) MIMO radar waveform design for binary hypothesis testing, and 2) active user detection in multiple access systems. The convergence tolerance for all iterative algorithms is set to  $\epsilon = 10^{-6}$ .

### A. Convergence and Runtime Analysis

We first assess the convergence behavior and computational efficiency of the proposed algorithms. We consider a MIMO sensing setup with  $N_t = N_r = 32$  antennas and a sequence length of  $T = 50$ . The SNR is set to 7 dB. We compare our proposed frameworks—FP-KLD (Algorithm 1), MM-KLD (Algorithm 2), and A-MM-KLD (Algorithm 3)—against the state-of-the-art benchmark, which is the MM-based algorithm proposed in [21].

Fig. 1 illustrates the evolution of the KLD objective function with respect to the number of iterations. Several key observations can be made regarding the convergence properties of the proposed schemes. First, all proposed algorithms exhibit a monotonic increase in the objective function, empirically validating our theoretical derivation that frames them as valid instances of the MM framework. Second, comparing the unaccelerated schemes, FP-KLD requires fewer iterations to converge than MM-KLD. This behavior directly corroborates our theoretical analysis in Section IV-A: FP-KLD utilizes a tight, anisotropic quadratic surrogate derived from the matrix fractional programming transform, whereas MM-KLD employs a nonhomogeneous relaxation. This relaxation based on Lemma 3 replaces the exact curvature with a conservative isotropic spectral bound, resulting in a looser surrogate and, consequently, a slower linear convergence rate. However, the proposed A-MM-KLD dramatically overcomes this limitation. By incorporating STEM, it effectively estimates the Jacobian of the fixed-point mapping, achieving a quasi-quadratic convergence rate. As shown in Fig. 1, A-MM-KLD converges

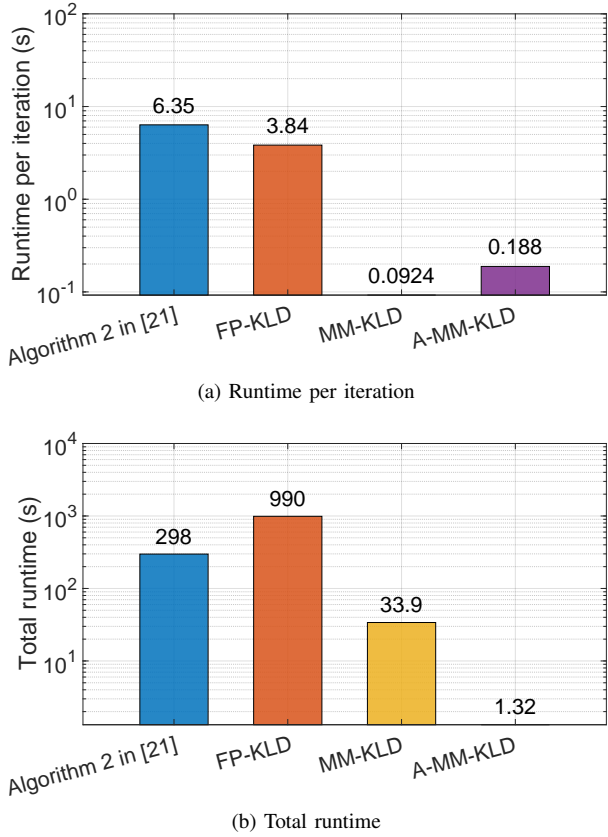


Fig. 2: Computational complexity comparison in terms of runtime. The proposed A-MM-KLD algorithm achieves orders-of-magnitude faster convergence than the benchmark [21] and FP-KLD methods.

rapidly requiring fewer iterations than the computationally heavier methods.

While iteration count is an important metric, the practical latency of an algorithm is determined by the total runtime, which is the product of the number of iterations and the per-iteration computation time. Fig. 2 presents a comprehensive runtime analysis.

Fig. 2a compares the average runtime required for a single iteration. Both the benchmark method [21] and our FP-KLD suffer from high per-iteration cost. This is because they both involve solving large-scale linear systems at every step, leading to a cubic computational complexity with respect to the problem dimension. In contrast, MM-KLD and A-MM-KLD reduce the per-iteration complexity by orders of magnitude. This substantial speedup is attributed to the nonhomogeneous relaxation, which yields a simple closed-form update for the waveform, thereby eliminating the need for computationally expensive matrix inversions or linear system solvers.

Fig. 2b displays the total runtime until convergence. The results highlight the superiority of the proposed A-MM-KLD framework. Although FP-KLD requires fewer iterations, its high per-iteration cost results in the longest total runtime. Conversely, while MM-KLD is extremely fast per iteration, its slow convergence rate leads to a moderate total runtime. A-MM-KLD effectively combines the best of both worlds: it

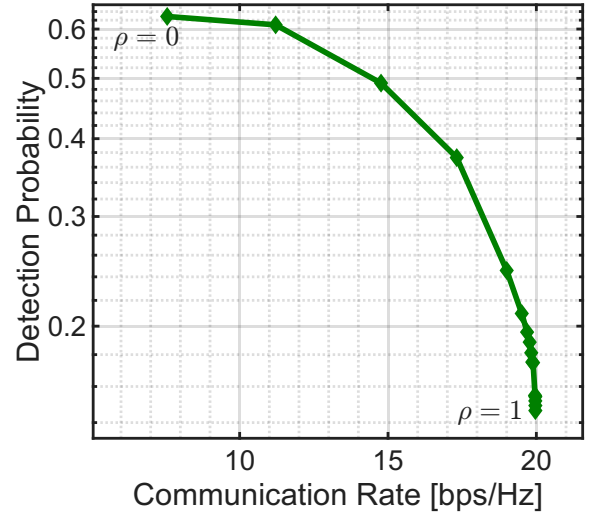


Fig. 3: Pareto boundary of the detection probability versus mutual information in the ISAC scenario. The trade-off is obtained by sweeping  $\rho$  from 0 to 1.

retains the low per-iteration complexity of the relaxed formulation while achieving rapid convergence through acceleration. Consequently, A-MM-KLD outperforms the state-of-the-art benchmark by several orders of magnitude in terms of total runtime, making it a highly scalable solution for large-scale antenna arrays.

### B. ISAC Pareto Boundary

Following the convergence and complexity analysis, we investigate the joint ISAC waveform design problem formulated in Section V-A by using the proposed framework. We evaluate the trade-off between the sensing capability and communication rate (MI) by varying the weighting parameter  $\rho$  in the objective function (59) from 0 to 1.

Fig. 3 illustrates the achievable performance region bounded by the Pareto frontier of the communication rate versus the detection probability (plotted on a logarithmic scale). As expected, a clear trade-off is observed between the two conflicting metrics. When  $\rho = 0$ , the optimization focuses solely on sensing, achieving the highest detection probability at the cost of reduced communication rate. Conversely, as  $\rho$  approaches 1, the design prioritizes MI, leading to higher data rates but degrading the detection reliability.

It is noteworthy that the proposed algorithm successfully traces the smooth Pareto curve without requiring any structural modifications to the solver. Since both KLD and MI terms are handled via a unified FP-based logic, our framework effectively balances the dual objectives. This result empirically confirms that the proposed method serves as a robust and scalable solution not only for pure sensing tasks but also for ISAC systems.

### C. Performance in Multiple Random Access

We next apply the proposed A-MM-KLD algorithm to the multiple random access scenario described in Section V-B. We

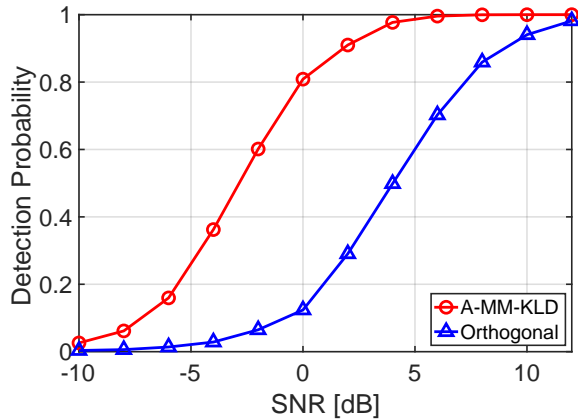


Fig. 4: Geometric mean of detection probabilities versus SNR. The sequence length is fixed at  $T = 8$ , and the threshold is set for  $\alpha = 10^{-3}$ . The proposed method significantly outperforms the orthogonal sequences by effectively mitigating MUI.

consider a system with  $K = 4$  devices, where both the transmitter and receiver are equipped with  $N_t = N_r = 4$  antennas. For detection, we employ the LRT based on the Neyman-Pearson criterion. The detection threshold  $\eta$  is determined numerically to satisfy a target probability of false alarm, set to  $\alpha = 10^{-3}$ . The performance metric is the geometric mean of the detection probabilities of all users, which ensures fairness and reflects the overall system reliability. We compare our optimized waveforms against conventional orthogonal sequences.

Fig. 4 presents the detection performance versus SNR with a fixed sequence length of  $T = 8$ . It is observed that the proposed A-MM-KLD algorithm yields a substantial performance gain over the orthogonal sequences across the entire SNR regime. This advantage stems from the fact that fixed orthogonal sequences do not account for the specific spatial covariance structures of the channels or the interference patterns. In contrast, our method explicitly maximizes the weighted sum of KLDs by jointly optimizing the waveforms to be robust against MUI generated by the random activity of other devices. Consequently, the proposed design achieves reliable detection even at lower SNR levels where the baseline fails.

Fig. 5 illustrates the detection performance versus the sequence length  $T$  at a fixed SNR of 8 dB. As expected, the detection probability improves as  $T$  increases for both schemes, since a longer duration provides more degrees of freedom to suppress interference and accumulate signal energy. However, the proposed algorithm demonstrates significantly faster saturation to perfect detection. Notably, in the regime of short sequence lengths, where the system is overloaded, the orthogonal sequences suffer severely from MUI. Conversely, the proposed waveforms maintain high detection capability even with limited temporal resources, highlighting the spectral efficiency and low-latency potential of our KLD-based design.

## VII. CONCLUSION

In this paper, we addressed the nonconvex problem of maximizing the KLD for hypothesis testing, a fundamental task in designing optimal sensing systems. We proposed an

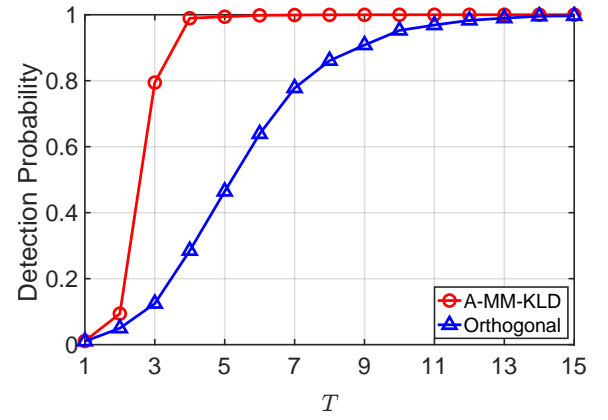


Fig. 5: Geometric mean of detection probabilities versus sequence length  $T$ . The SNR is fixed at 8 dB with  $\alpha = 10^{-3}$ . The proposed design achieves near-perfect detection even with limited sequence lengths, demonstrating its suitability for low-latency random access.

efficient iterative framework, termed FP-KLD, which leverages a sequence of transforms. This approach systematically reformulates the intractable objective into a sequence of simple concave quadratic subproblems, each of which can be solved efficiently by analyzing its KKT conditions, leading to a Sylvester equation. To further enhance computational efficiency and make the method scalable, we developed an advanced FP-KLD algorithm using nonhomogeneous relaxation. This variant circumvents the high computational cost, resulting in a simple, closed-form update for the sensing waveform at each iteration.

Additionally, we provided a rigorous justification for the monotonic convergence of our algorithms by establishing their equivalence to the MM and BCA frameworks. Furthermore, we demonstrated how the performance of these fixed-point iterations can be substantially improved using standard acceleration techniques. We also illustrated the framework's flexibility by applying it to the ISAC and the multiple random access scenarios.

The numerical results provided comprehensive insights into the trade-offs among the proposed schemes. First, FP-KLD achieved fastest convergence, empirically validating the tightness of the FP-derived surrogate. Second, MM-KLD significantly reduced the per-iteration computational burden via nonhomogeneous relaxation, though this came at the cost of an increased number of iterations. The A-MM-KLD algorithm successfully combined these advantages; it yielded a remarkable reduction in total runtime compared to state-of-the-art methods while guaranteeing monotonic convergence. Our proposed methods also showed strong performance in the joint ISAC waveform design and the random access scenarios.

Several directions exist for extending the proposed framework. One promising way is to apply the A-MM-KLD principle to accelerate MIMO optimizers. In particular, when advanced multiple access schemes (e.g., rate-splitting multiple access) are considered, the resulting objective functions become nonsmooth and highly nonconvex [14], [25], [50], often leading to slow convergence of existing algorithms. Adapting

our acceleration technique to these scenarios could significantly alleviate the computational burden, paving a way for real-time implementation of complex interference management techniques.

## REFERENCES

- [1] S. Kullback and R. A. Leibler, "On information and sufficiency," *Ann. Math. Statist.*, vol. 22, no. 1, pp. 79–86, 1951.
- [2] N. Merhav, G. Kaplan, A. Lapidot, and S. Shamai Shitz, "On information rates for mismatched decoders," *IEEE Trans. Inf. Theory*, vol. 40, no. 6, pp. 1953–1967, 1994.
- [3] H. Chernoff, "A measure of asymptotic efficiency for tests of a hypothesis based on the sum of observations," *Ann. Math. Statist.*, vol. 23, no. 4, pp. 493–507, 1952.
- [4] M. Al-Jarrah, E. Alsusa, and C. Masouros, "A unified performance framework for integrated sensing-communications based on KL-divergence," *IEEE Trans. Wireless Commun.*, vol. 22, no. 12, pp. 9390–9411, 2023.
- [5] Z. Fei, S. Tang, X. Wang, F. Xia, F. Liu, and J. A. Zhang, "Revealing the trade-off in ISAC systems: The KL divergence perspective," *IEEE Wireless Commun. Lett.*, 2024.
- [6] Y. Kloob, M. Al-Jarrah, E. Alsusa, and C. Masouros, "Novel KLD-based resource allocation for integrated sensing and communication," *IEEE Trans. Signal Process.*, vol. 72, pp. 2292–2307, 2024.
- [7] K. Shen and W. Yu, "Fractional programming for communication systems—Part I: Power control and beamforming," *IEEE Trans. Signal Process.*, vol. 66, no. 10, pp. 2616–2630, 2018.
- [8] ———, "Fractional programming for communication systems—Part II: Uplink scheduling via matching," *IEEE Trans. Signal Process.*, vol. 66, no. 10, pp. 2631–2644, 2018.
- [9] P. Stoica, J. Li, and Y. Xie, "On probing signal design for MIMO radar," *IEEE Trans. Signal Process.*, vol. 55, no. 8, pp. 4151–4161, 2007.
- [10] I. Bekkerman and J. Tabrikian, "Target detection and localization using MIMO radars and sonars," *IEEE Trans. Signal Process.*, vol. 54, no. 10, pp. 3873–3883, 2006.
- [11] M. Bell, "Information theory and radar waveform design," *IEEE Trans. Inf. Theory*, vol. 39, no. 5, pp. 1578–1597, 1993.
- [12] Z. Zhu, S. Kay, and R. S. Raghavan, "Information-theoretic optimal radar waveform design," *IEEE Signal Process. Lett.*, vol. 24, no. 3, pp. 274–278, 2017.
- [13] K. Shen, W. Yu, L. Zhao, and D. P. Palomar, "Optimization of MIMO device-to-device networks via matrix fractional programming: A minorization–maximization approach," *IEEE/ACM Trans. Netw.*, vol. 27, no. 5, pp. 2164–2177, 2019.
- [14] J. Park, J. Choi, N. Lee, W. Shin, and H. V. Poor, "Rate-splitting multiple access for downlink MIMO: A generalized power iteration approach," *IEEE Trans. Wireless Commun.*, vol. 22, no. 3, pp. 1588–1603, 2023.
- [15] S. S. Christensen, R. Agarwal, E. De Carvalho, and J. M. Cioffi, "Weighted sum-rate maximization using weighted MMSE for MIMO-BC beamforming design," *IEEE Trans. Wireless Commun.*, vol. 7, no. 12, pp. 4792–4799, 2008.
- [16] Q. Shi, M. Razaviyayn, Z.-Q. Luo, and C. He, "An iteratively weighted mmse approach to distributed sum-utility maximization for a MIMO interfering broadcast channel," *IEEE Trans. Signal Process.*, vol. 59, no. 9, pp. 4331–4340, 2011.
- [17] Y. Yang and R. S. Blum, "MIMO radar waveform design based on mutual information and minimum mean-square error estimation," *IEEE Trans. Aerosp. Electron. Syst.*, vol. 43, no. 1, pp. 330–343, 2007.
- [18] L. Wang, H. Wang, Y. Cheng, Y. Qin, and P. V. Brennan, "Adaptive waveform design for maximizing resolvability of targets," in *Proc. 18th Int. Conf. Digit. Signal Process. (DSP)*. IEEE, 2013, pp. 1–6.
- [19] E. Grossi and M. Lops, "Space-time code design for MIMO detection based on Kullback-Leibler divergence," *IEEE Trans. Inf. Theory*, vol. 58, no. 6, pp. 3989–4004, 2012.
- [20] L. Wang, W. Zhu, Y. Zhang, Q. Liao, and J. Tang, "Multi-target detection and adaptive waveform design for cognitive MIMO radar," *IEEE Sens. J.*, vol. 18, no. 24, pp. 9962–9970, 2018.
- [21] B. Tang, Y. Zhang, and J. Tang, "An efficient minorization maximization approach for MIMO radar waveform optimization via relative entropy," *IEEE Trans. Signal Process.*, vol. 66, no. 2, pp. 400–411, 2018.
- [22] B. Tang, M. M. Naghsh, and J. Tang, "Relative entropy-based waveform design for MIMO radar detection in the presence of clutter and interference," *IEEE Trans. Signal Process.*, vol. 63, no. 14, pp. 3783–3796, 2015.
- [23] F. Liu, Y.-F. Liu, A. Li, C. Masouros, and Y. C. Eldar, "Cramér-Rao bound optimization for joint radar-communication beamforming," *IEEE Trans. Signal Process.*, vol. 70, pp. 240–253, 2022.
- [24] J. Choi, J. Park, N. Lee, and A. Alkhateeb, "Joint and robust beamforming framework for integrated sensing and communication systems," *IEEE Trans. Wireless Commun.*, vol. 23, no. 11, pp. 17602–17618, 2024.
- [25] N. Kim, J. Han, J. Choi, A. Alkhateeb, C.-B. Chae, and J. Park, "Integrated sensing and communications in downlink FDD MIMO without CSI feedback," *IEEE Trans. Wireless Commun.*, pp. 1–1, 2025.
- [26] Y. Chen, Y. Feng, X. Li, L. Zhao, and K. Shen, "Fast fractional programming for multi-cell integrated sensing and communications," *IEEE Trans. Wireless Commun.*, vol. 24, no. 8, pp. 6797–6812, 2025.
- [27] A. M. Haimovich, R. S. Blum, and L. J. Cimini, "MIMO radar with widely separated antennas," *IEEE Sig Process. Mag.*, vol. 25, no. 1, pp. 116–129, 2007.
- [28] A. De Maio and M. Lops, "Design principles of MIMO radar detectors," *IEEE Trans. Aerosp. Electron. Syst.*, vol. 43, no. 3, pp. 886–898, 2007.
- [29] H. L. Van Trees, *Detection, Estimation, and Modulation Theory, Part I: Detection, Estimation, and Linear Modulation Theory*. John Wiley & Sons, 2004.
- [30] T. M. Cover and J. A. Thomas, *Elements of Information Theory*. USA: Wiley-Interscience, 2006.
- [31] S. M. Kay, *Fundamentals of Statistical Signal Processing: Estimation Theory*. Prentice-Hall, Inc., 1993.
- [32] K. Shen, Z. Zhao, Y. Chen, Z. Zhang, and H. V. Cheng, "Accelerating quadratic transform and WMMSE," *IEEE J. Sel. Areas Commun.*, 2024.
- [33] R. A. Horn and C. R. Johnson, *Matrix Analysis*. Cambridge university press, 2012.
- [34] S. Boyd and L. Vandenberghe, *Convex Optimization*. Cambridge university press, 2004.
- [35] K.-w. E. Chu, "The solution of the matrix equations  $AXB - CXD = E$  and  $(YA - DZ, YC - BZ) = (E, F)$ ," *Linear Algebra Appl.*, vol. 93, pp. 93–105, 1987.
- [36] F. De Terán, B. Iannazzo, F. Poloni, and L. Robol, "Solvability and uniqueness criteria for generalized Sylvester-type equations," *Linear Algebra Appl.*, vol. 542, pp. 501–521, 2018.
- [37] R. Varadhan and C. Roland, "Simple and globally convergent methods for accelerating the convergence of any EM algorithm," *Scand. J. Stat.*, vol. 35, no. 2, pp. 335–353, 2008.
- [38] Y. Sun, P. Babu, and D. P. Palomar, "Majorization-minimization algorithms in signal processing, communications, and machine learning," *IEEE Trans. Signal Process.*, vol. 65, no. 3, pp. 794–816, 2016.
- [39] G. H. Golub and C. F. Van Loan, *Matrix Computations*. JHU press, 2013.
- [40] W. H. Press, S. A. Teukolsky, W. T. Vetterling, and B. P. Flannery, *Numerical Recipes: The Art of Scientific Computing*, 3rd ed. Cambridge University Press, 2007.
- [41] D. R. Hunter and K. Lange, "A tutorial on MM algorithms," *Amer. Statist.*, vol. 58, no. 1, pp. 30–37, 2004.
- [42] K. Lange, *Numerical Analysis for Statisticians*. Springer, 1999.
- [43] B. T. Polyak, "Some methods of speeding up the convergence of iteration methods," *USSR Comput. Math. Math. Phys.*, vol. 4, no. 5, pp. 1–17, 1964.
- [44] Y. Nesterov, "A method for solving the convex programming problem with convergence rate  $\mathcal{O}(1/k^2)$ ," in *Sov. Math. Dokl.*, vol. 269, 1983, p. 543.
- [45] J. Steffensen, "Remarks on iteration," *Scand. Actuar. J.*, vol. 1933, no. 1, pp. 64–72, 1933.
- [46] Y. Nievergelt, "Aitken's and Steffensen's accelerations in several variables," *Numer. Math.*, vol. 59, no. 1, pp. 295–310, 1991.
- [47] A. R. Chiriyath, B. Paul, and D. W. Bliss, "Radar-communications convergence: Coexistence, cooperation, and co-design," *IEEE Trans. Cognitive Comm. and Networking*, vol. 3, no. 1, pp. 1–12, 2017.
- [48] D. Chu, "Polyphase codes with good periodic correlation properties," *IEEE Trans. Inf. Theory*, vol. 18, no. 4, pp. 531–532, 1972.
- [49] R. Frank, S. Zadoff, and R. Heimiller, "Phase shift pulse codes with good periodic correlation properties," *IEEE Trans. Inf. Theory*, vol. 8, no. 6, pp. 381–382, 1962.
- [50] N. Kim, I. P. Roberts, and J. Park, "Splitting messages in the dark: Rate-splitting multiple access for FDD massive MIMO without CSI feedback," *IEEE Trans. Wireless Commun.*, vol. 24, no. 4, pp. 3320–3332, 2025.